Surface-Initiated Photoinduced ATRP: Mechanism, Oxygen Tolerance and Temporal Control during the Synthesis of Polymer Brushes

Wenqing Yan,[1] Sajjad Dadashi-Silab,[2] Krzysztof Matyjaszewski,[2] Nicholas D. Spencer,[1]* Edmondo M. Benetti[1,3]**

[1]Laboratory of Surface Science and Technology, Department of Materials, Swiss Federal Institute of Technology (ETH Zürich), Vladimir-Prelog-Weg 1-5/10, CH-8093 Zurich, Switzerland

[2]Department of Chemistry, Carnegie Mellon University, 4400 Fifth Avenue, Pittsburgh, PA 15213, USA

[3]Swiss Federal Laboratories for Materials Science and Technology (Empa), Lerchenfeldstrasse 5, CH-9014, St. Gallen, Switzerland

This document is the accepted manuscript version of the following article:
Yan, W., Dadashi-Silab, S., Matyjaszewski, K., Spencer, N. D., & Benetti, E. M. (2020). Surface-initiated photoinduced ATRP: mechanism, oxygen tolerance, and temporal control during the synthesis of polymer brushes. Macromolecules, 53(8), 2801-2810. https://doi.org/10.1021/acs.macromol.0c00333

KEYWORDS: polymer brushes; controlled radical polymerization; thin films; surface functionalization; coatings

Abstract

Surface-initiated, photoinduced atom transfer radical polymerization (SI-photoATRP) enables the controlled and rapid synthesis of compositionally diverse polymer brushes over large areas, by employing very small reaction volumes, under ambient conditions and without the need for prior deoxygenation of monomer mixtures. The concentration of copper species, and the type and content of amine-based ligands determine the mechanism of SI-photoATRP, regulate the kinetics of polymer-brush growth, and govern the tolerance of this polymer-grafting method toward oxygen. Despite mechanistic analogies with the corresponding solution processes, the intrinsic, highly confined nature of SI-photoATRP leads to significant differences from polymerizations within homogeneous systems. This is especially important to attain controlled/living polymerization and temporal control over polymer-brush growth using UV light as a trigger.

Introduction

Over the past decade, there have been significant advancements in photochemically stimulated reversible deactivation radical polymerization (RDRP) methods. These have involved the application of light for inducing and/or catalyzing controlled polymer growth.[1-4] Prominent examples include photoinduced electron transfer reversible-addition fragmentation radical polymerization (PET-RAFT),[5-7] photoinduced atom transfer radical polymerization (photoATRP)[8-11] and photocatalyzed metal-free ATRP.[12-16]

Focusing on photoATRP, this polymerization technique presents several advantages with respect to other ATRP processes. These include the possibility of temporal control over polymer chain growth, which is regulated by illumination time, enhanced tolerance of photoATRP toward oxygen,[17-21] and the reduction in the amount of catalyst necessary to attain a controlled polymerization.[9]

All these unique features rely on the intrinsic mechanism of photoATRP, which mainly involves the (re)generation of $Cu^{I}X$/L-based activators under light irradiation. Upon excitation of initially present $Cu^{II}X_2$/L ($[Cu^{II}X_2/L]^*$ in Scheme 1a), a single-electron transfer with an electron donor, typically a free ligand (L), generates $Cu^{I}X$/L activators. Thus, in photoATRP, electron donors act as reducing agents similar to activator regenerated by electron transfer (ARGET) ATRP. To a lesser extent, alkyl halide initiators (RX) can additionally undergo homolytic cleavage upon irradiation, generating a halide radical (X·) and a carbon-centered radical (R·) that can initiate/propagate chains in the presence of monomer.[10, 22]

Mechanistic studies of photoATRP reveal that in the presence of oxygen, $Cu^{I}X$/L generates $Cu^{II}X(O_2)$/L species, which in the excited state can recombine with L (or an electron donor), yielding oxidized species (L_{ox}), as well as regenerating $Cu^{I}X$/L activators.[17-19] In a closed reaction system not deoxygenated, and with a limited amount of dissolved oxygen, this process continues until essentially all oxygen has been consumed.[17, 23] Thus, the presence of excess

ligand (or other electron donors) guarantees the efficient regeneration of an activator, and imparts to photoATRP a degree of tolerance towards environmental conditions, circumventing the need for tedious deoxygenation procedures prior to polymerization.

The translation of these features into the controlled synthesis of polymer brushes, via surface-initiated photoATRP (SI-photoATRP), would substantially broaden the applicability of RDRP methods for the creation of functional surfaces, and the modification of a variety of materials. The tolerance of SI-photoATRP to environmental conditions is of special relevance for polymer grafting from large substrates.[24-26] These include sensors,[27-30] cell-sensitive and tissue-engineering platforms[31-37] or catalytic supports.[38-40] Scaling up polymer-brush synthesis using classical ATRP processes from such substrates would require the use of extremely large reaction volumes, with the necessity for maintaining inert conditions for relatively long reaction times. Such processes would additionally require the use of large quantities of catalyst. All these factors hamper the translation of commonly applied surface-initiated ATRP (SI-ATRP) methods into technologically relevant processes.

With the aim of investigating the mechanism of SI-photoATRP, in this study we focus on exploring how the presence of a grafting surface affects those parameters that have already been identified as crucial for photoATRP in solution. During SI-photoATRP, the concentration of Cu^{II} species initially added to the reaction mixture as well as the type and amount of ligand determine polymer-brush growth rate, and the degree of control over the polymerization. These parameters additionally regulate the tolerance of the polymerization toward oxygen.

We employed a reaction setup in which initiator-functionalized substrates were uniformly covered with a few microliters of monomer/catalyst solutions (Scheme 1). We demonstrated that under constant UV illumination, SI-photoATRP enables the generation of extremely uniform polymethacrylate brush films over very large areas, without the need for prior deoxygenation of the reaction mixtures or the presence of an inert atmosphere.

Due to the minimal reaction volumes employed, coupled to the intrinsically confined nature of SI-photoATRP, only a brief period of UV irradiation was sufficient to consume dissolved oxygen in the system, and trigger a progressive, controlled brush-growth over several hours in complete darkness. This unique feature redefines the concept of temporal control during photoinduced RDRP, which is typically regulated by switching on/off the light source, in the particular case of systems where polymer growth takes place under highly confined environments. Attaining polymer growth without the need for continuous UV irradiation thus highlights SI-photoATRP as an extremely energetically efficient polymerization technique. This is particularly well-suited for the generation of coatings on substrates where limited light penetration can be achieved, as is the case for the in situ modification of implants, or the fabrication of adhesive films.

Experimental Section

Materials. Dimethylformamide (DMF, extra pure, Fisher Chemical), acetone (> 99.8%, VWR Chemicals), tetrahydrofuran (THF, > 99.5%, VWR Chemicals), triethylamine (TEA, ⩾99%, Merck), 2-bromoisobutryl bromide (BiBB, 98%, Sigma-Aldrich), 3-(aminopropyl)triethoxysilane (APTES, 99%, Acros), copper(II) bromide ($CuBr_2$, 99.99%, Aldrich), tris(2-pyridylmethyl)amine (TPMA, 98%, Sigma-Aldrich), tris[2-(dimethylamino)ethyl]amine (Me_6TREN, 99%, abcr GmbH), tetrabutylammonium fluoride (TBAF, 1M in THF, Aldrich), iron(III) bromide ($FeBr_3$, 98%, Sigma-Aldrich), tetrabutylammonium bromide (TBABr, >99%, Fluka), 1,1,4,7,7-pentamethyldiethylenetriamine (PMDETA, 99%, Aldrich-Fine Chemicals), 1,1,4,7,10,10-hexamethyltriethylenetetramine (HMTETA, 97%, Aldrich-Fine Chemicals), 2,2'-bipyridyl (bpy, >=99%, Sigma-Aldrich), ethylenediaminetetraacetic acid (EDTA, 99.995%, Sigma-

Aldrich), and sodium bromide (NaBr, >=99.0%, Sigma-Aldrich) were used as received. Silicon wafers were purchased from Si-Mat (Landsberg, Germany).

Methyl methacrylate (MMA, Sigma-Aldrich), oligo[(ethylene glycol) methyl ether methacrylate] (OEGMA, Mn ~ 480 g mol^{-1}, Sigma-Aldrich), 2-(trimethylsilyloxy)ethyl methacrylate (HEMATMS, 96%, Sigma-Aldrich), 2-(dimethylamino)ethyl methacrylate (DMAEMA, 98%, Aldrich-Fine Chemicals), 2-hydroxyethyl methacrylate (HEMA, 97%, abcr GmbH), and glycidyl methacrylate (GMA, Sigma-Aldrich) were purified by passing through a basic alumina column to remove the inhibitor before use.

Variable-Angle Spectroscopic Ellipsometry (VASE). The values of dry thickness of polymer brushes (T_{dry}) were measured using a M-2000F John Woollam variable angle spectroscopic ellipsometer (VASE, SENTECH Instruments GmbH) equipped with a He-Ne laser source (λ = 633 nm, J.A. Woollam Co., Lincoln, NE). Amplitude (Ψ) and phase (Δ) components were recorded using focusing lenses at 70 ° from the surface normal as a function of wavelength (350−800 nm). Fitting of the raw data was performed based on a layered model using bulk dielectric functions for Si and SiO_2 (software WVASE32, LOT Oriel GmbH, Darmstadt, Germany). The polymer-brush layers were analyzed on the basis of a Cauchy model: $n = A + B\,\lambda^{-2}$, where n is the refractive index, λ is the wavelength and A and B were assumed to be 1.45 and 0.01, respectively, as values for transparent organic films.

Size Exclusion Chromatography (SEC). Polymer brushes grafted from 8-inch silicon wafer by SI-photoATRP were detached after overnight treatment in a 0.05 M THF solution of TBAF at 60 °C. After the reaction, the solvent was removed in rotary evaporator and the solid was filtered and re-dissolved in THF.

SEC was performed on a Viskotek GPCMax system (Malvern) equipped with two PFG linear M columns (PSS), eluting the samples in THF at a rate of 1 mL min^{-1} at room temperature. The values of M_n and *PDI* of de-grafted polymer brushes were obtained using the signal originating

from a refractive index (RI) detector, and a conventional calibration employing narrowly dispersed PMMA standards.

Preparation of ATRP Initiator Layer on SiO_x Substrates. Silicon substrates with an area of 4 cm^2 were cleaned for 20 minutes in *piranha* solution (3:1 mixture (v/v) of H_2SO_4 and H_2O_2), and subsequently rinsed with ultrapure water (Millipore Milli-Q grade) and ethanol. APTES was subsequently deposited on SiO_x surfaces by vapour deposition, in a desiccator that was kept under vacuum for 3 hours. After this, ATRP-initiator layers were obtained by incubating APTES-bearing substrates in a 0.12 M DCM solution of BiBB, containing 0.12 M TEA. The reaction was carried out for 2 hours at room temperature, and the samples were subsequently washed with DCM, and finally dried under a stream of N_2.

Surface-Initiated Photoinduced ATRP. SI-photoATRP was conducted in a Stratalinker UV Crosslinker 2400 (Stratagene, La Jolla, CA, USA) equipped with 6 UV lamps having λ_{max} = 365 nm, and generating a power of 1.5 mW cm^{-2}. The reactions were carried out at room temperature and in the presence of oxygen. SiO_x substrates previously functionalized with ATRP initiator were placed in a glass petri dish, covered with 10 μL cm^{-2} of polymerization mixture and a glass slide. The sandwiched substrates were irradiated for the desired time, rinsed with solvent and finally dried under a stream of N_2.

Results and Discussion

The mechanism of SI-photoATRP was initially explored by analyzing the parameters that had been previously identified as the principal determinants for the controlled growth of polymers in the corresponding solution processes.[9-11, 22-23] In particular, the effects of catalyst concentration (expressed as the amount of Cu^{II} species initially added), and the content and type of ligand (L) on the synthesis of polymer brushes by SI-photoATRP were investigated. As illustrated in Scheme 1a, the amine-based L substantially contributes to the generation of

$Cu^{I}X/L$ species, and prevents accumulation of $Cu^{II}X_2/L$ deactivators throughout the grafting process, following an overall mechanism that is reminiscent of ARGET ATRP.[41-42]

In the presence of UV irradiation $Cu^{II}X_2/L$ can be photo-excited to $[Cu^{II}X_2/L]^*$, which is subsequently quenched by L in solution, generating $Cu^{I}X/L$ and a radical cation ($L^{\cdot+}$). Hence, a concentration of L beyond the stoichiometric amount necessary to form Cu^{II} complexes is typically required to efficiently generate activators and enable a steady initiation and propagation.

Besides the type and amount of L, the concentration of Cu^{II} species present in solution determines the degree of control over the polymerization process. This is especially relevant in the case of polymer-brush synthesis from macroscopic surfaces, where the concentration of catalyst at the brush-growing front regulates deactivation efficiency, and the extent of irreversible termination reactions between propagating grafts.[43-46] This latter phenomenon becomes important in determining the growth of brush films via SI-ATRP processes. On the one hand, a relatively high local concentration of radicals is generated, since they are virtually all confined to the surface. On the other hand, just a limited amount of Cu^{II} species is produced in the medium through the ATRP equilibrium, and as a result of termination processes, owing to the overall extremely low concentration of initiating/propagating sites.[47]

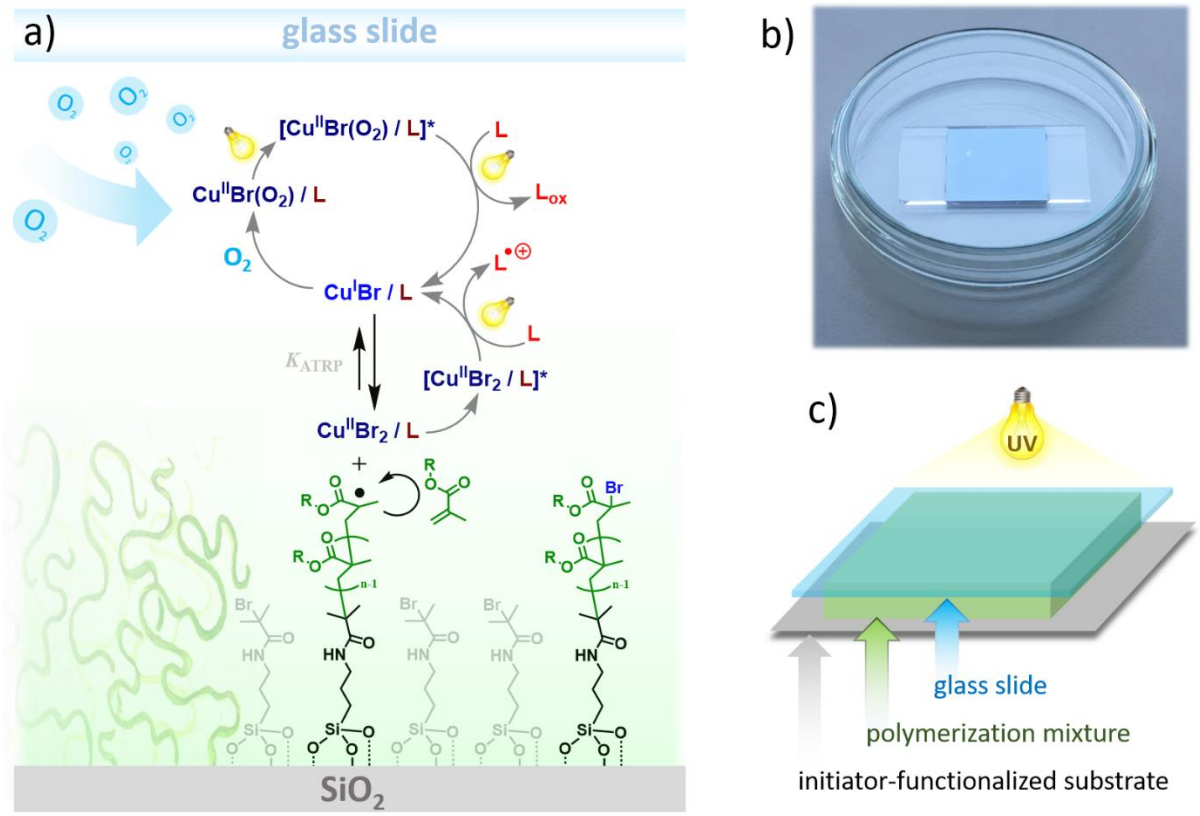

Scheme 1. (a) Proposed mechanism of SI-photoATRP; (b, c) reaction setup employed for the synthesis of polymethacrylate brushes by SI-photoATRP, including an ATRP initiator-functionalized SiO_x substrate covered with a polymerization mixture and sandwiched with a glass slide.

Effect of Ligand

The synthesis of poly[oligo(ethylene glycol) methacrylate] (POEGMA) and poly(methyl methacrylate) (PMMA) brushes by SI-photoATRP was investigated. In both cases, polymer grafting was performed from ATRP-initiator-functionalized SiO_x surfaces, onto which 1 µL cm^{-2} 1:1 (v/v) monomer:dimethylformamide (DMF) mixtures were applied, without deoxygenation. The samples were subsequently covered with a glass slide, and irradiated under environmental conditions (no inert atmosphere) by a UV light source with λ_{max} = 365 nm, and an intensity of 1.5 mW cm^{-2}. Four different ligands, yielding Cu-based catalysts with a broad range of activities were tested, namely tris[2-(dimethylamino)ethyl]amine (Me_6TREN), tris(2-pyridylmethyl)amine (TPMA), N,N,N′,N″,N″-pentamethyldiethylenetriamine (PMDETA) and

1,1,4,7,10,10-hexamethyltriethylenetetramine (HMTETA). Two concentrations of $CuBr_2$ were used for each ligand type, 0.44 mM (100 ppm) and 5 mM (~1100 ppm), and different relative amounts of L were tested, generating mixtures with [$CuBr_2$]:[L] of 1:2, 1:4 and 1:6.

As summarized in Table 1 and 2, when Me_6TREN and TPMA were used as ligands, relatively thick POEGMA and PMMA brushes were obtained after just one hour of UV irradiation, in all cases exceeding 20-30 nm of dry thickness (T_{dry}), as measured by variable angle spectroscopic ellipsometry (VASE). It is important to emphasize that, in contrast to previously reported data focusing on photoATRP of acrylates in solution,[10-11, 18-19] when Me_6TREN and TPMA were used as ligands a decrease in [$CuBr_2$]:[L] did not translate into a faster polymerization from the surface, as similar values of T_{dry} for different brush films typically indicate a comparable molar mass of the corresponding grafted polymers.[48-54] This result agrees well with the data reported by Mosnàček et al.[17], who suggested that the rate of photoATRP of methacrylates might be independent of the excess of ligand present in the reaction.

Table 1. SI-photoATRP Of OEGMA Performed By Varying L, [$CuBr_2$], and [$CuBr_2$]:[L].

Monomer and Ligand	[$CuBr_2$]	[$CuBr_2$]:[L]	Time (h)	T_{dry} (nm)
OEGMA Me_6TREN	100 ppm	1: 2	1	36.8 ± 0.4
	100 ppm	1: 4	1	39.4 ± 1.5
	100 ppm	1: 6	1	40.5 ± 2.3
OEGMA Me_6TREN	5 mM	1: 2	1	51.6 ± 0.1
	5 mM	1: 4	1	44.1 ± 0.9
	5 mM	1: 6	1	47.7 ± 0.2
OEGMA TPMA	100 ppm	1: 2	1	45.6 ± 0.2
	100 ppm	1: 4	1	48.5 ± 2.3
	100 ppm	1: 6	1	49.3 ± 0.2
OEGMA TPMA	5 mM	1: 2	1	23.4 ± 1.1
	5 mM	1: 4	1	26.3 ± 1.2
	5 mM	1: 6	1	28.4 ± 0.1
OEGMA PMDETA	100 ppm	1: 2	3	0.8 ± 0.1
	100 ppm	1: 4	3	0.9 ± 0.1
	100 ppm	1: 6	3	1.2 ± 0.1
OEGMA PMDETA	5 mM	1: 2	3	8.7 ± 0.2
	5 mM	1: 4	3	41.5 ± 0.4

	5 mM	1: 6	3	42.2 ± 0.3
OEGMA HMTETA	100 ppm	1: 2	3	0.8 ± 0.1
	100 ppm	1: 4	3	0.9 ± 0.1
	100 ppm	1: 6	3	0.9 ± 0.1
OEGMA HMTETA	5 mM	1: 2	3	1.9 ± 0.3
	5 mM	1: 4	3	6.1 ± 0.1
	5 mM	1: 6	3	20.5 ± 0.7

Significantly different results were obtained when PMDETA and HMTETA were used as L. Both ligands generated much less active Cu catalysts, characterized by markedly lower values of ATRP equilibrium constant (K_{ATRP}).[55] In both these cases, 100 ppm of $CuBr_2$ was not sufficient to enable the grafting of POEGMA and PMMA brushes, even after 3 hours of irradiation, while films with a measurable thickness were obtained by increasing [$CuBr_2$] to 5 mM. At higher concentration of Cu, a clear dependency of T_{dry} on the relative content of L was recorded. In particular, the thickness of POEGMA brushes increased from 8.7 ± 0.2 nm when [$CuBr_2$]:[PMDETA] was 1:2, to 42.2 ± 0.3 nm when four fold excess of PMDETA with respect to $CuBr_2$ was applied. Similarly, T_{dry} of POEGMA increased from 1.9 ± 0.3 to 20.5 ± 0.7 nm when [$CuBr_2$]:[HMTETA] was shifted from 1:2 to 1:6, while analogous trends, although with overall lower values of thickness, were recorded for SI-photoATRP of MMA (Table 2).

Table 2. SI-photoATRP Of MMA Performed By Varying L, [$CuBr_2$], and [$CuBr_2$]:[L].

Monomer and Ligand	[$CuBr_2$]	[$CuBr_2$]:[L]	Time (h)	T_{dry} (nm)
MMA Me_6TREN	100 ppm	1: 2	1	34.8 ± 0.2
	100 ppm	1: 4	1	41.0 ± 0.3
	100 ppm	1: 6	1	42.1 ± 0.8
MMA Me_6TREN	5 mM	1: 2	1	28.2 ± 0.2
	5 mM	1: 4	1	24.0 ± 0.3
	5 mM	1: 6	1	26.5 ± 0.4
MMA TPMA	100 ppm	1: 2	1	5.8 ± 0.2
	100 ppm	1: 4	1	9.4 ± 0.1
	100 ppm	1: 6	1	6.4 ± 0.2
MMA TPMA	5 mM	1: 2	1	5.7 ± 0.3
	5 mM	1: 4	1	4.7 ± 0.1
	5 mM	1: 6	1	5.6 ± 0.1

MMA PMDETA	100 ppm	1: 2	3	0.7 ± 0.1
	100 ppm	1: 4	3	0.9 ± 0.2
	100 ppm	1: 6	3	1.0 ± 0.3
MMA PMDETA	5 mM	1: 2	3	6.1 ± 0.3
	5 mM	1: 4	3	6.3 ± 0.1
	5 mM	1: 6	3	9.6 ± 0.1
MMA HMTETA	100 ppm	1: 2	3	0.7 ± 0.1
	100 ppm	1: 4	3	0.7 ± 0.1
	100 ppm	1: 6	3	0.8 ± 0.1
MMA HMTETA	5 mM	1: 2	3	1.3 ± 0.1
	5 mM	1: 4	3	4.9 ± 0.2
	5 mM	1: 6	3	10.5 ± 0.1

Effect of Catalyst Concentration

Kinetic studies of polymer-brush growth shed further light on the mechanism of SI-photoATRP. To analyze the thickening rates of POEGMA brushes, and assess their dependency on the variation of reaction parameters, we focused on catalytic systems involving Me_6TREN and TPMA, which provided the fastest polymerizations according to the results reported in Tables 1 and 2.

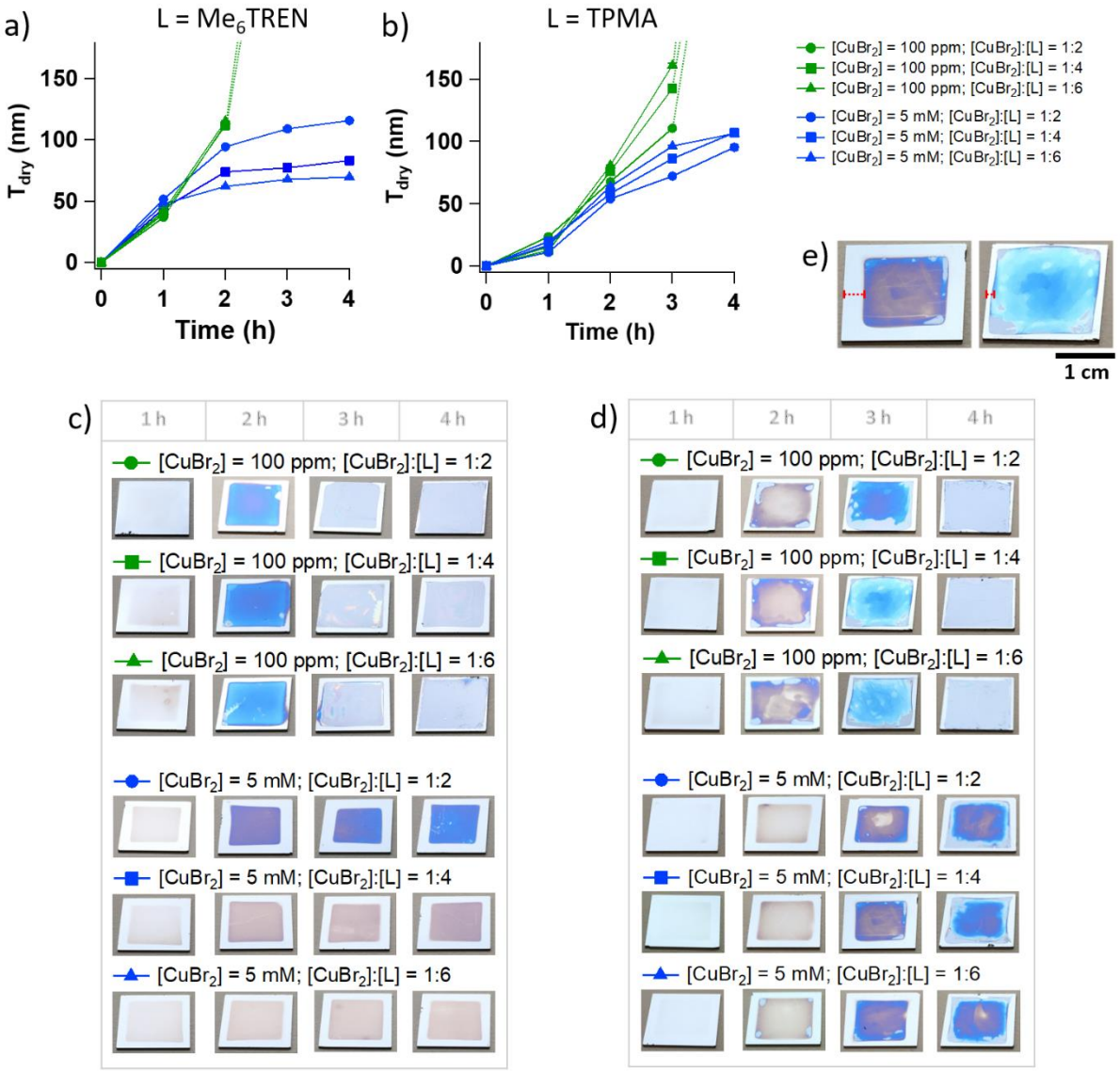

Figure 1. (a, b) POEGMA brush-growth rates recorded by measuring T_{dry} of polymer brushes following different UV irradiation times during SI-photoATRP. The polymerization mixtures comprised 1:1 (v/v) DMF:OEGMA, 100 ppm (green traces) and 5 mM (blue traces) $CuBr_2$, and different contents of L, corresponding to $[CuBr_2]$:[L] of 1:2, 1:4 and 1:6. (a) L = Me_6TREN; (b) L = TPMA. (c, d) Pictures of representative substrates following POEGMA brush synthesis using Me_6TREN and TPMA as ligands, respectively, are reported. The brush films show different colours due to thickness-dependent light interference, while inhomogeneous layers are highlighted by areas presenting patches of different colours. (e) Pictures depicting POEGMA brushes synthesized after 4 h of SI-photoATRP using TPMA as ligand, 5 mM (left side) and 100 ppm of $CuBr_2$ (right side), while maintaining in both cases $[CuBr_2]$:[L] of 1:4.

As highlighted by comparing the growth profiles reported in Figure 1a and 1b, when POEGMA was grafted by using Me_6TREN as a ligand, brush thickness steadily increased during the early

stages of UV irradiation, reaching values of T_{dry} between 40 and 50 nm after 1 h of polymerization (Figure 1a). In contrast, for catalytic systems involving TPMA as a ligand, a discontinuity in the slope of brush-growth profiles was recorded after 1 h of exposure to UV, for all values of [$CuBr_2$] and [$CuBr_2$]:[L] tested (Figure 1b). The differences observed along the brush-thickening profiles at the beginning of the polymerization were due to the different rates of photoinduced reduction of $Cu^{II}X/L$ species between the two ligands. Since Me_6TREN contains four reactive aliphatic amine moieties, the rate of photoreduction of Cu^{II}-based species was significantly higher than that with TPMA, which has one alkyl-amine moiety and three pyridinic groups (Figure S1).[11]

Hence, oxygen consumption at the early stages of reaction through complexation with photogenerated $Cu^{I}X/L$ (Scheme 1a) was slower with TPMA, and a certain induction period was observed before a progressive POEGMA brush growth could be attained.

As expected from the initial polymerizations summarized in Table 1 and 2, an evident increment in polymerization rate with increase in ligand concentration was not observed, in the case of either Me_6TREN or TPMA. In contrast, significantly faster brush-thickening rates were recorded for relatively low initial contents of $CuBr_2$. In particular, the growth of POEGMA brushes assumed a rather uncontrolled behavior after a few hours of UV irradiation when [$CuBr_2$] was set to 100 ppm, and the entire reaction completely gelled after 2 and 3 h, with Me_6TREN and TPMA ligands, respectively. Under these conditions, T_{dry} of POEGMA films reached values > 1 μm, and the films were generally inhomogeneous. In addition, the fitting of VASE data when [$CuBr_2$] = 100 ppm often provided unreliable results both during the synthesis of PMMA and POEGMA brushes.

The uncontrolled nature of SI-photoATRP at relatively low values of [$CuBr_2$] was further confirmed by synthesizing PMMA brushes over large areas, and subsequently analyzing chemically detached chains by size-exclusion chromatography (SEC). As reported in Figure 2,

after 3 h of UV irradiation, PMMA brushes with T_{dry} between 20 and 30 nm were obtained from 4-inch silicon wafers, with [$CuBr_2$] = 5 mM (Figure 2a) or 100 ppm (Figure 2b). Although applying the two different formulations resulted in similar thicknesses of PMMA brushes, at lower catalyst concentration (100 ppm) polymers with a significantly larger dispersity ($Đ$) = 2.5 was obtained, whereas increasing [$CuBr_2$] to 5 mM decreased $Đ$ to 1.3.

Hence, at relatively low concentration of Cu species, SI-photoATRP was very fast, as previously reported by Laun *et al.* for SI-photoATRP of various acrylates.[56] However, in the case of polymethacrylate brushes, the grafting process was less controlled, showing features reminiscent of surface-initiated conventional free radical polymerization (SI-FRP).

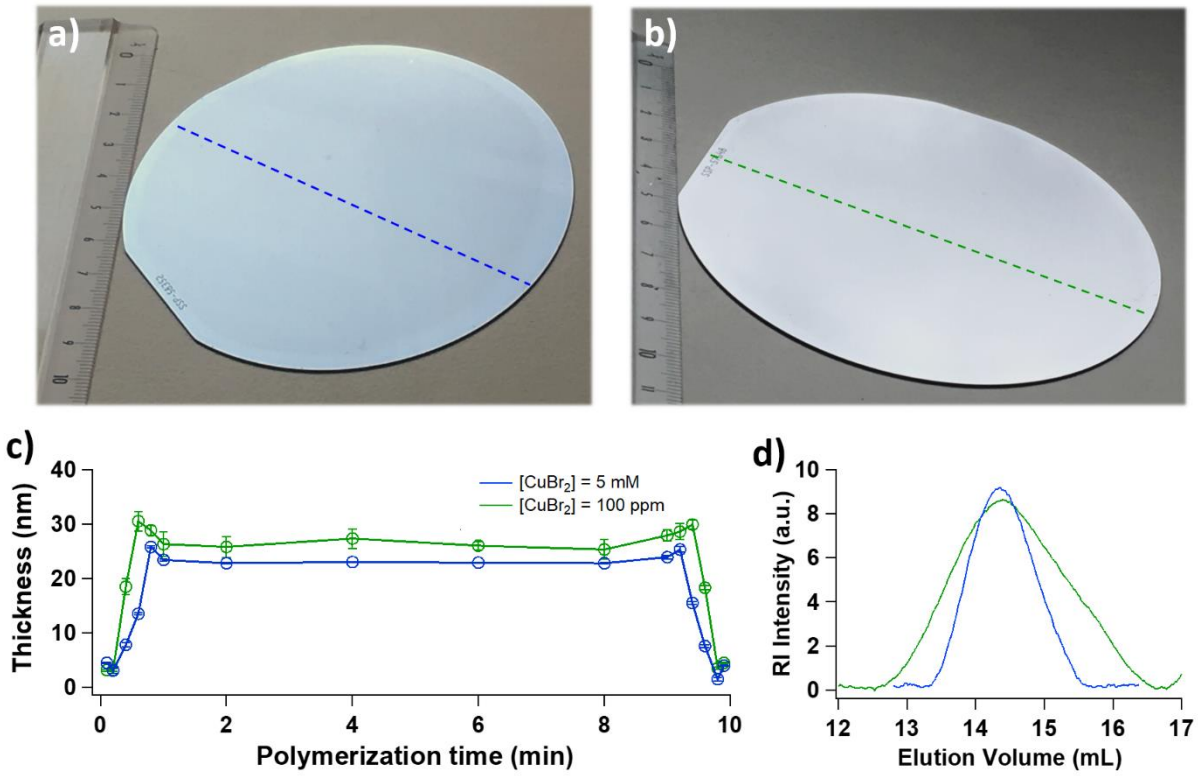

Figure 2. PMMA brushes synthesized by SI-photoATRP from ATRP initiator-functionalized, 4-inch silicon wafers, and using different polymerization mixtures. (a) 1:1 (v/v) MMA:DMF, 5 mM $CuBr_2$, [$CuBr_2$]:[L] = 1:4. (b) 1:1 (v/v) MMA:DMF, 100 ppm $CuBr_2$, [$CuBr_2$]:[L] = 1:4. (c) After 3 h of UV irradiation T_{dry} of PMMA brushes lay between 20 and 30 nm, as measured by VASE. (d) SEC analysis of detached PMMA brushes provided M_n of 75 kDa and $Đ$ of 2.5 when 100 ppm of $CuBr_2$ were used, while an M_n of 101 kDa and $Đ$ of 1.3 were obtained when 5 mM $CuBr_2$ were applied.

A similar result was recently reported by Wang *et al.*,[47] when reduction of catalyst concentration in the synthesis of PMMA brushes by SI-ARGET ATRP from initiator-functionalized SiO_2 nanoparticles (NPs) resulted in a loss of control over the grafting process. This was ascribed to inefficient deactivation and inhomogeneous initiation, leading to the concomitant generation of sparsely grafted polymer-brush shells. Interestingly, during grafting from NPs, a value of $[CuBr_2] > 10$ ppm was the threshold above which the growth of brushes became controlled. In contrast, when PMMA was grafted from macroscopic surfaces through SI-photoATRP, a relatively higher concentration of catalyst was needed to attain a progressive and controlled growth of narrowly dispersed polymer chains. We believe that the observed differences were mainly due to the geometry of the reaction setup used to generate brushes from large, macroscopic surfaces, and the absence of stirring within the extremely small reaction volumes (layer thickness). Both these factors determined a relatively low concentration of Cu^{II} species at the brush-growing front.

The interface between the propagating chains and the surrounding medium, where the deactivation by $Cu^{II}X/L$ species takes place, is in fact limited to the area of the substrate (significantly lower than the interfacial area between NPs and the surrounding medium). Additionally, the absence of stirring reduced the local concentration of deactivator. Hence, as a result of the intrinsic design of SI-photoATRP applied from flat substrates, a relatively high concentration of catalyst is necessary to guarantee an efficient deactivation of radicals, and thus a controlled progressive polymer growth.

The application of a catalytic system consisting of 5 mM $CuBr_2$ and TPMA as ligand thus enabled the synthesis from extremely large substrates of thick and compositionally different brushes, including poly(hydroxyethyl methacrylate) (PHEMA), poly[2-(dimethylamino)ethyl

methacrylate] (PDMAEMA), poly(glycidyl methacrylate) (PGMA) and polystyrene (PS) brushes (Figure S2).

The different behavior of SI-photoATRP when relatively "low" and "high" catalyst concentrations were applied, additionally influenced the effect plaid by diffusing oxygen on the grafting process. Considering the polymerization setup designed for these experiments (Schemes 1b and 1c), with an initiator-bearing substrate and a glass slide sandwiching a thin liquid film with an average thickness of ~ 10 μm, the constant dissolution of oxygen through the open sides of this setup substantially hampered polymer growth in the areas of the substrate close to the edges. In these regions, T_{dry} was < 5 nm, regardless of the polymerization time or other reaction parameters. In contrast, in areas further away from the edges oxygen could be consumed through complexation by Cu^{I}/L, followed by reaction with excess of ligand to yield oxidized species (Scheme 1a).[17-18]

It is important to emphasize that, while the edges could be clearly distinguished when SI-photoATRP was performed with 5 mM $CuBr_2$ (typically ~ 5 mm on a 2×2 cm^2 substrate), a significant reduction in the areas where polymer grafting did not occur was evident for [$CuBr_2$] = 100 ppm (Figure 1e). Under these conditions, the growth of polymer brushes was accompanied by an increase in viscosity of the reaction mixture, which is typical of SI-FRP. Hence, this phenomenon presumably decreased the rate of oxygen diffusion through the edges of the sandwiched substrates, leading to a reduction in the non-grafted areas.

Temporal Control of SI-photoATRP

Having established the critical parameters for the mechanism of SI-photoATRP, and its tolerance toward ambient conditions, we subsequently investigated how polymer grafting could be temporally regulated by modulating the UV illumination.

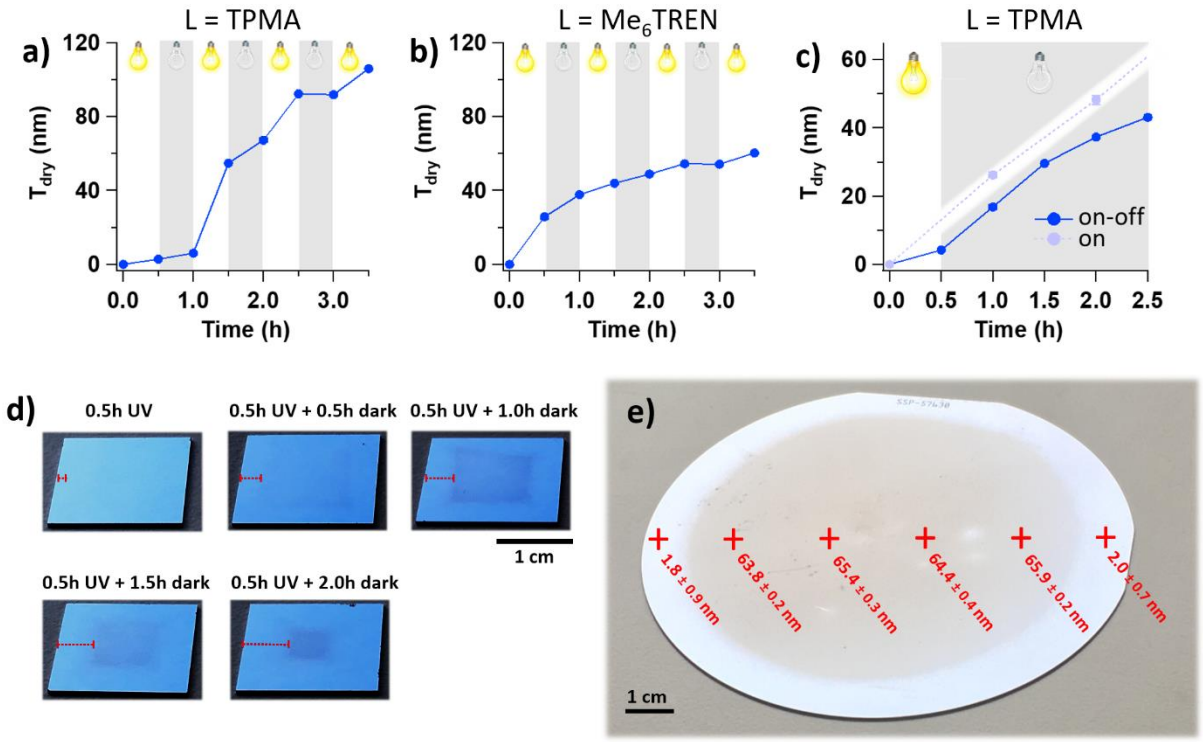

Figure 3. POEGMA brush growth by SI-photoATRP was monitored by VASE, alternating periods of UV illumination with intervals in the dark, using polymerization mixtures including 1:1 (v/v) OEGMA:DMF, 5 mM $CuBr_2$, and $CuBr_2$]:[L] of 1:4. (a) L = TPMA. (b) L = Me_6TREN. (c) POEGMA brush growth was monitored by VASE, subjecting ATRP-initiator-functionalized substrates covered with a polymerization mixture to UV irradiation for 30 min, followed by 2 h in the dark. The growth of POEGMA brushes during SI-photoATRP under constant UV irradiation is also reported as a pale-blue, dashed profile. (d) Digital photographs of PEOGMA brushes synthesized by SI-photoATRP from 2×2 cm^2 ATRP initiator-functionalized substrates after 0.5 h of UV illumination, followed by different periods during which the substrates were kept in the dark. The size of the edge where brush growth is hindered due to oxygen diffusion is highlighted with a red marker. (e) POEGMA brushes grafted by SI-photoATRP from an ATRP-initiator-functionalized, 4 inch silicon wafer covered by polymerization mixture and subsequently subjected to 30 min of UV irradiation and 2 h of darkness.

Control over polymer chain growth by switching on and off the light source that triggers the generation of active catalyst was extensively studied for homogeneous photoATRP in solution.[9, 11, 17, 57-59] Under certain conditions, polymerization in the absence of light could also continue.[60-61]

Temporal control over SI-photoATRP was studied for OEGMA (1:1 v/v in DMF), using 5 mM $CuBr_2$ and 30 mM TPMA, by alternating periods of 30 min of UV illumination and darkness.

As shown in Figure 3a, the first irradiation step resulted in a moderate thickening of the films, presumably due to initial oxygen consumption, as observed in the brush-growth rates recorded under continuous UV illumination (Figure 1b). A subsequent period of darkness did not stop the brush growth. In contrast, POEGMA brushes showed a slight but significant thickening, analogous to that recorded during the first 30 min under UV irradiation.

The second UV illumination step was mirrored by a significant increment in brush thickness, which reached a T_{dry} of almost 50 nm. During the subsequent 30 min of darkness, the brush growth continued without a sharp response to the absence of UV light by a rapid termination.

When Me_6TREN was used as ligand within otherwise analogous polymerization mixtures, temporal control over POEGMA brush growth by switching UV light alternatively on and off was not attained. In fact, brush-thickening rates recorded during UV illumination were similar to those observed in the darkness (Figure 3b).

These results indicated that achieving excellent temporal control over SI-photoATRP by modulating UV irradiation is a more challenging task than for solution polymerizations. This could be due to the large excess of Cu catalysts over alkyl halides during SI-photoATRP. In homogeneous systems, the content of Cu catalyst is typically much lower than that of alkyl halides, and radical termination in the dark can consume all available activators, halting the chain growth.[60,61] Therefore, in the absence of UV light, photo(re)generation of Cu^{I}-based activators does not occur and polymer growth stops. In contrast, in SI-photoATRP the amount of Cu catalysts is much larger than that of alkyl halides.[62] Thus, a small fraction of terminated chains cannot significantly affect the concentration of Cu^{I} species and polymerization continues also in the dark periods. Interestingly, more efficient temporal control over brush growth was observed with TPMA as ligand. The relatively lower observed rate of photoreduction of $Cu^{II}Br_2$/TPMA (Figure S1) produces lower concentration of Cu^{I}-based activators that can be comparable to a fraction of terminated chains growing from the surface.

Despite the observed limitations in gaining precise temporal control over the grafting process, the unavoidable brush growth taking place in the absence of light, and following a relatively short period of UV illumination, emerged as an appealing feature of SI-photoATRP. This could be especially convenient, if this surface functionalization method was applied for generating coatings or adhesive layers from spatially confined or light-sensitive supports, where continuous illumination over long periods of time is undesirable or cannot be easily achieved. POEGMA brush growth under "dark conditions" could be monitored by initially irradiating an initiator-bearing substrate covered with the same polymerization mixture used for the "on-off" experiments for 30 min, and subsequently measuring the brush-thickening rate by VASE while the reaction setup was kept in the dark for several hours (Figure 3c).

As illustrated in Figure 3c, when UV light was applied, increase of T_{dry} showed a slight initial induction period, due to oxygen consumption in the mixture. In contrast, during the subsequent period in the dark, a progressive film thickening was recorded over ~ 1.5 h, following a kinetics similar to that recorded during continuous UV illumination. After this relatively long stage, film thickening slowed down, significantly deviating from the growth rates observed when the UV light was continuously applied.

In the absence of UV light that (re)generates Cu^{I} species, the diffusion of oxygen from the sides of the sample led to a progressive increment in the size of the edges where polymerization was retarded, which increased from ~ 0.1 cm, after 0.5 h, to ~ 0.7 cm, after 2.5 h in the dark. Due to this phenomenon, the areas covered with propagating brushes gradually decreased in size, with the POEGMA films covering just the center of the substrates after several hours without UV illumination (Figure 3d). This drawback could be easily overcome by increasing the size of the entire substrate, thus minimizing the observed edge-effect caused by oxygen diffusion and catalyst deactivation. As shown in Figure 3e, when POEGMA brushes were grafted from

a 4-inch silicon wafer following a similar sequence of UV illumination and darkness, an extremely large area (many tens of cm^2) covered with a uniformly thick brush were obtained.

Conclusions

The mechanistic analysis of SI-photoATRP highlights the parameters determining its controlled character, the kinetics of polymer-brush growth, and the tolerance of this surface modification method toward ambient conditions.

A relatively high concentration of catalyst was required to attain the synthesis of narrowly dispersed polymer brushes. In contrast, when just 100 ppm of $CuBr_2$ was used, inefficient deactivation of radicals caused an extremely fast polymer-brush growth, which followed a behavior typical of free radical polymerization.

Contrary to what was previously observed in the case of the corresponding solution processes, polymer-brush growth rates were independent of the content of free ligand, especially for ligands generating catalysts with relatively high K_{ATRP}, such as TPMA and Me_6TREN. In the cases of less ATRP-active catalysts with HMTETA and PMDETA ligands, brush thickness increased with the excess of ligand, confirming the central role of alkyl amines as reducing agents for Cu^{II} species in the presence of UV irradiation.

The extremely low amount of alkyl halide functions compared to Cu-based catalyst during SI-photoATRP strongly influenced the possibility of controlling the grafting process temporally, by modulating the exposure to UV light. Following a relatively short period of illumination, a non-negligible film growth was always recorded, suggesting that polymer grafts were continuously activated by the excess of Cu^{I} species. Hence, a progressive and controlled growth of polymer brushes can be attained in the dark, just following a short, initial stage of UV illumination, during which oxygen was consumed and Cu^{I}-based activators were generated. Uniformly thick brush films could be generated over large areas, suggesting an extremely

efficient method to fabricate functional coatings from light-sensitive substrates, or from spatially confined supports where just a limited dose of UV light can be applied.

Supporting Information

The Supporting Information is available free of charge at XXX

Kinetics of photoreduction of $Cu^{II}X/L$; additional VASE characterization.

Author Information

Corresponding Authors:

*Email: matyjaszewski@cmu.edu

*Email: nicholas.spencer@mat.ethz.ch

*Email: edmondo.benetti@mat.ethz.ch

Acknowledgments

We thank Prof. Katharina Maniura (Empa) for the valuable discussions. This work was financially supported by European Union's Horizon 2020 research and innovation program (grant agreement No 669562) and by the National Science Foundation (DMR 1501324).

Competing interests

The authors declare no competing interests.

References

1. Dadashi-Silab, S.; Doran, S.; Yagci, Y., Photoinduced Electron Transfer Reactions for Macromolecular Syntheses. *Chem. Rev.* **2016,** *116* (17), 10212-10275.

2. Shanmugam, S.; Xu, J. T.; Boyer, C., Photocontrolled Living Polymerization Systems with Reversible Deactivations through Electron and Energy Transfer. *Macromol. Rapid Commun.* **2017,** *38* (13).

3. Ribelli, T. G.; Lorandi, F.; Fantin, M.; Matyjaszewski, K., Atom Transfer Radical Polymerization: Billion Times More Active Catalysts and New Initiation Systems. *Macromol. Rapid Commun.* **2019,** *40* (1).

4. Pan, X. C.; Tasdelen, M. A.; Laun, J.; Junkers, T.; Yagci, Y.; Matyjaszewski, K., Photomediated controlled radical polymerization. *Prog. Polym. Sci.* **2016,** *62*, 73-125.

5. Jung, K.; Xu, J. T.; Zetterlund, P. B.; Boyer, C., Visible-Light-Regulated Controlled/Living Radical Polymerization in Miniemulsion. *ACS Macro Lett.* **2015,** *4* (10), 1139-1143.

6. Shanmugam, S.; Xu, J. T.; Boyer, C., Exploiting Metalloporphyrins for Selective Living Radical Polymerization Tunable over Visible Wavelengths. *J. Am. Chem. Soc.* **2015,** *137* (28), 9174-9185.

7. Shanmugam, S.; Xu, J. T.; Boyer, C., Light-Regulated Polymerization under Near-Infrared/Far-Red Irradiation Catalyzed by Bacteriochlorophyll a. *Angew. Chem. Int. Ed.* **2016,** *55* (3), 1036-1040.

8. Tasdelen, M. A.; Uygun, M.; Yagci, Y., Photoinduced Controlled Radical Polymerization. *Macromol. Rapid Commun.* **2011,** *32* (1), 58-62.

9. Konkolewicz, D.; Schröder, K.; Buback, J.; Bernhard, S.; Matyjaszewski, K., Visible Light and Sunlight Photoinduced ATRP with ppm of Cu Catalyst. *ACS Macro Lett.* **2012,** *1* (10), 1219-1223.

10. Ribelli, T. G.; Konkolewicz, D.; Bernhard, S.; Matyjaszewski, K., How are Radicals (Re)Generated in Photochemical ATRP? *J. Am. Chem. Soc.* **2014,** *136* (38), 13303-13312.

11. Anastasaki, A.; Nikolaou, V.; Zhang, Q.; Burns, J.; Samanta, S. R.; Waldron, C.; Haddleton, A. J.; McHale, R.; Fox, D.; Percec, V.; Wilson, P.; Haddleton, D. M., Copper(II)/Tertiary Amine Synergy in Photoinduced Living Radical Polymerization: Accelerated Synthesis of ω-Functional and α,ω-Heterofunctional Poly(acrylates). *J. Am. Chem. Soc.* **2014,** *136* (3), 1141-1149.

12. Treat, N. J.; Sprafke, H.; Kramer, J. W.; Clark, P. G.; Barton, B. E.; de Alaniz, J. R.; Fors, B. P.; Hawker, C. J., Metal-Free Atom Transfer Radical Polymerization. *J. Am. Chem. Soc.* **2014,** *136* (45), 16096-16101.

13. Miyake, G. M.; Theriot, J. C., Perylene as an Organic Photocatalyst for the Radical Polymerization of Functionalized Vinyl Monomers through Oxidative Quenching with Alkyl Bromides and Visible Light. *Macromolecules* **2014,** *47* (23), 8255-8261.

14. Allushi, A.; Jockusch, S.; Yilmaz, G.; Yagci, Y., Photoinitiated Metal-Free Controlled/Living Radical Polymerization Using Polynuclear Aromatic Hydrocarbons. *Macromolecules* **2016,** *49* (20), 7785-7792.

15. Theriot, J. C.; Lim, C. H.; Yang, H.; Ryan, M. D.; Musgrave, C. B.; Miyake, G. M., Organocatalyzed Atom Transfer Radical Polymerization Driven by Visible Light. *Science* **2016,** *352* (6289), 1082-1086.

16. Pan, X. C.; Fang, C.; Fantin, M.; Malhotra, N.; So, W. Y.; Peteanu, L. A.; Isse, A. A.; Gennaro, A.; Liu, P.; Matyjaszewskit, K., Mechanism of Photoinduced Metal-Free Atom Transfer Radical Polymerization: Experimental and Computational Studies. *J. Am. Chem. Soc.* **2016,** *138* (7), 2411-2425.

17. Mosnacek, J.; Eckstein-Andicsova, A.; Borska, K., Ligand effect and oxygen tolerance studies in photochemically induced copper mediated reversible deactivation radical polymerization of methyl methacrylate in dimethyl sulfoxide. *Polym. Chem.* **2015,** *6* (13), 2523-2530.

18. Borska, K.; Moravcikova, D.; Mosnacek, J., Photochemically Induced ATRP of (Meth)Acrylates in the Presence of Air: The Effect of Light Intensity, Ligand, and Oxygen Concentration. *Macromol. Rapid Commun.* **2017,** *38* (13).

19. Bondarev, D.; Borska, K.; Soral, M.; Moravcikova, D.; Mosnacek, J., Simple Tertiary Amines as Promotors in Oxygen Tolerant Photochemically Induced ATRP of Acrylates. *Polymer* **2019,** *161*, 122-127.

20. Yang, Q. Z.; Lalevee, J.; Poly, J., Development of a Robust Photocatalyzed ATRP Mechanism Exhibiting Good Tolerance to Oxygen and Inhibitors. *Macromolecules* **2016,** *49* (20), 7653-7666.

21. Pan, X. C.; Fantin, M.; Yuan, F.; Matyjaszewski, K., Externally Ccontrolled Atom Transfer Radical Polymerization. *Chem. Soc. Rev.* **2018,** *47* (14), 5457-5490.

22. Frick, E.; Anastasaki, A.; Haddleton, D. M.; Barner-Kowollik, C., Enlightening the Mechanism of Copper Mediated PhotoRDRP via High-Resolution Mass Spectrometry. *J. Am. Chem. Soc.* **2015,** *137* (21), 6889-6896.

23. Liarou, E.; Anastasaki, A.; Whitfield, R.; Iacono, C. E.; Patias, G.; Engelis, N. G.; Marathianos, A.; Jones, G. R.; Haddleton, D. M., Ultra-low volume oxygen tolerant photoinduced Cu-RDRP. *Polym. Chem.* **2019,** *10* (8), 963-971.

24. Dunderdale, G. J.; Urata, C.; Miranda, D. F.; Hozumi, A., Large-Scale and Environmentally Friendly Synthesis of pH-Responsive Oil-Repellent Polymer Brush Surfaces under Ambient Conditions. *ACS Appl. Mater. Interfaces* **2014,** *6* (15), 11864-11868.

25. Dunderdale, G. J.; England, M. W.; Urata, C.; Hozumi, A., Polymer Brush Surfaces Showing Superhydrophobicity and Air-Bubble Repellency in a Variety of Organic Liquids. *ACS Appl. Mater. Interfaces* **2015,** *7* (22), 12220-12229.

26. Sato, T.; Dunderdale, G. J.; Urata, C.; Hozumi, A., Sol-Gel Preparation of Initiator Layers for Surface-Initiated ATRP: Large-Scale Formation of Polymer Brushes Is Not a Dream. *Macromolecules* **2018,** *51* (24), 10065-10073.

27. Schuwer, N.; Tercier-Waeber, M. L.; Danial, M.; Klok, H. A., Voltammetric Detection of Hg^{2+} Using Peptide-Functionalized Polymer Brushes. *Austr. J. Chem.* **2012,** *65* (8), 1104-1109.

28. Fortin, N.; Klok, H. A., Glucose Monitoring Using a Polymer Brush Modified Polypropylene Hollow Fiber-based Hydraulic Flow Sensor. *ACS Appl. Mater. Interfaces* **2015,** *7* (8), 4631-4640.

29. Badoux, M.; Billing, M.; Klok, H. A., Polymer Brush Interfaces for Protein Biosensing Prepared by Surface-Initiated Controlled Radical Polymerization. *Polym. Chem.* **2019**, 10 (23), 2925-2951.

30. Christau, S.; Genzer, J.; von Klitzing, R., Polymer Brush/Metal Nanoparticle Hybrids for Optical Sensor Applications: from Self-Assembly to Tailored Functions and Nanoengineering. *Z. Phys. Chem.* **2015,** *229* (7-8), 1089-1117.

31. Krishnamoorthy, M.; Hakobyan, S.; Ramstedt, M.; Gautrot, J. E., Surface-Initiated Polymer Brushes in the Biomedical Field: Applications in Membrane Science, Biosensing, Cell Culture, Regenerative Medicine and Antibacterial Coatings. *Chem. Rev.* **2014,** *114* (21), 10976-11026.

32. Moroni, L.; Gunnewiek, M. K.; Benetti, E. M., Polymer Brush Coatings Regulating Cell Behavior: Passive Interfaces Turn into Active. *Acta Biomater.* **2014,** *10* (6), 2367-2378.

33. Klein Gunnewiek, M.; Di Luca, A.; Bollemaat, H. Z.; van Blitterswijk, C. A.; Vancso, G. J.; Moroni, L.; Benetti, E. M., Creeping Proteins in Microporous Structures: Polymer

Brush-Assisted Fabrication of 3D Gradients for Tissue Engineering. *Adv. Health. Mater.* **2015,** *4* (8), 1169–1174.

34. Benetti, E. M.; Gunnewiek, M. K.; van Blitterswijk, C. A.; Vancso, G. J.; Moroni, L., Mimicking Natural Cell Environments: Design, Fabrication and Application of Bio-Chemical Gradients on Polymeric Biomaterial Substrates. *J. Mater. Chem. B* **2016,** *4* (24), 4244-4257.

35. Gunnewiek, M. K.; Ramakrishna, S. N.; di Luca, A.; Vancso, G. J.; Moroni, L.; Benetti, E. M., Stem-Cell Clinging by a Thread: AFM Measure of Polymer-Brush Lateral Deformation. *Adv. Mater. Interfaces* **2016,** *3* (3), 1500456.

36. Nagase, K.; Hatakeyama, Y.; Shimizu, T.; Matsuura, K.; Yamato, M.; Takeda, N.; Okano, T., Thermoresponsive Cationic Copolymer Brushes for Mesenchymal Stem Cell Separation. *Biomacromolecules* **2015,** *16* (2), 532-540.

37. Morgese, G.; Cavalli, E.; Rosenboom, J. G.; Zenobi-Wong, M.; Benetti, E. M. Cyclic Polymer Grafts That Lubricate and Protect Damaged Cartilage. *Angew. Chem. Int. Edit.* **2018,** *57* (6), 1621-1626.

38. Costantini, F.; Benetti, E. M.; Reinhoudt, D. N.; Huskens, J.; Vancso, G. J.; Verboom, W., Enzyme-Functionalized Polymer Brush Films on the Inner Wall of Silicon-Glass Microreactors with Tunable Biocatalytic activity. *Lab Chip* **2010,** *10* (24), 3407-3412.

39. Costantini, F.; Benetti, E. M.; Tiggelaar, R. M.; Gardeniers, H. J. G. E.; Reinhoudt, D. N.; Huskens, J.; Vancso, G. J.; Verboom, W., A Brush-Gel/Metal-Nanoparticle Hybrid Film as an Efficient Supported Catalyst in Glass Microreactors. *Chem. Eur. J.* **2010,** *16* (41), 12406-12411.

40. Rafti, M.; Brunsen, A.; Fuertes, M. C.; Azzaroni, O.; Soler-Illia, G. J. A. A., Heterogeneous Catalytic Activity of Platinum Nanoparticles Hosted in Mesoporous

Silica Thin Films Modified with Polyelectrolyte Brushes. *ACS Appl. Mater. Interfaces* **2013,** *5* (18), 8833-8840.

41. Jakubowski, W.; Min, K.; Matyjaszewski, K., Activators Regenerated by Electron Transfer for Atom Transfer Radical Polymerization of Styrene. *Macromolecules* **2006,** *39* (1), 39-45.

42. Jakubowski, W.; Matyjaszewski, K., Activators Regenerated by Electron Transfer for Atom-Transfer Radical Polymerization of (Meth)acrylates and Related Block Copolymers. *Angew. Chem. Int. Ed.* **2006,** *45* (27), 4482-4486.

43. Cheng, N.; Azzaroni, O.; Moya, S.; Huck, W. T. S., The Effect of $[Cu^{I}]/[Cu^{II}]$ Ratio on the Kinetics and Conformation of Polyelectrolyte Brushes by Atom Transfer Radical Polymerization. *Macromol. Rapid Commun.* **2006,** *27* (19), 1632-1636.

44. Matyjaszewski, K.; Miller, P. J.; Shukla, N.; Immaraporn, B.; Gelman, A.; Luokala, B. B.; Siclovan, T. M.; Kickelbick, G.; Vallant, T.; Hoffmann, H.; Pakula, T., Polymers at Interfaces: Using Atom Transfer Radical Polymerization in the Controlled Growth of Homopolymers and Block Copolymers from Silicon Surfaces in the Absence of Untethered Sacrificial Initiator. *Macromolecules* **1999,** *32* (26), 8716-8724.

45. Dehghani, E. S.; Du, Y. H.; Zhang, T.; Ramakrishna, S. N.; Spencer, N. D.; Jordan, R.; Benetti, E. M., Fabrication and Interfacial Properties of Polymer Brush Gradients by Surface-Initiated Cu(0)-Mediated Controlled Radical Polymerization. *Macromolecules* **2017,** *50* (6), 2436-2446.

46. Zhou, D. P.; Gao, X.; Wang, W. J.; Zhu, S. P., Termination of Surface Radicals and Kinetic Modeling of ATRP Grafting from Flat Surfaces by Addition of Deactivator. *Macromolecules* **2012,** *45* (3), 1198-1207.

47. Wang, Z. Y.; Yan, J. J.; Liu, T.; Wei, Q. B.; Li, S. P.; Olszewski, M.; Wu, J. N.; Sobieski, J. L.; Fantin, M.; Bockstaller, M. R.; Matyjaszewski, K., Control of Dispersity

and Grafting Density of Particle Brushes by Variation of ATRP Catalyst Concentration. *ACS Macro Lett.* **2019,** *8* (7), 859-864.

48. Milner, S. T.; Witten, T. A.; Cates, M. E., A Parabolic Density Profile for Grafted Polymers. *Europhys. Lett.* **1988,** *5* (5), 413-418.

49. Milner, S. T.; Witten, T. A.; Cates, M. E., Theory of the Grafted Polymer Brush. *Macromolecules* **1988,** *21* (8), 2610-2619.

50. Benetti, E. M.; Kang, C. J.; Mandal, J.; Divandari, M.; Spencer, N. D., Modulation of Surface-Initiated ATRP by Confinement: Mechanism and Applications. *Macromolecules* **2017,** *50* (15), 5711-5718.

51. Kang, C.; Crockett, R. M.; Spencer, N. D., Molecular-Weight Determination of Polymer Brushes Generated by SI-ATRP on Flat Surfaces. *Macromolecules* **2014,** *47*, 269-275.

52. Kang, C. J.; Ramakrishna, S. N.; Nelson, A.; Cremmel, C. V. M.; Stein, H. V.; Spencer, N. D.; Isa, L.; Benetti, E. M., Ultrathin, Freestanding, Stimuli-Responsive, Porous Membranes from Polymer Hydrogel-Brushes. *Nanoscale* **2015,** *7* (30), 13017-13025.

53. Patil, R. R.; Turgman-Cohen, S.; Srogl, J.; Kiserow, D.; Genzer, J., Direct Measurement of Molecular Weight and Grafting Density by Controlled and Quantitative Degrafting of Surface-Anchored Poly(methyl methacrylate). *ACS Macro Lett.* **2015,** *4* (2), 251-254.

54. Patil, R. R.; Turgman-Cohen, S.; Srogl, J.; Kiserow, D.; Genzer, J., On-Demand Degrafting and the Study of Molecular Weight and Grafting Density of Poly(methyl methacrylate) Brushes on Flat Silica Substrates. *Langmuir* **2015,** *31* (8), 2372-2381.

55. Wang, Y.; Kwak, Y.; Buback, J.; Buback, M.; Matyjaszewski, K., Determination of ATRP Equilibrium Constants under Polymerization Conditions. *ACS Macro Lett.* **2012,** *1* (12), 1367-1370.

56. Laun, J.; Vorobii, M.; de los Santos Pereira, A.; Pop-Georgievski, O.; Trouillet, V.; Welle, A.; Barner-Kowollik, C.; Rodriguez-Emmenegger, C.; Junkers, T., Surface Grafting via Photo-Induced Copper-Mediated Radical Polymerization at Extremely Low Catalyst Concentrations. *Macromol. Rapid Commun.* **2015,** *36* (18), 1681-1686.

57. Zhang, T.; Chen, T.; Amin, I.; Jordan, R., ATRP with a Light Switch: Photoinduced ATRP Using a Household Fluorescent Lamp. *Polym. Chem.* **2014,** *5* (16), 4790-4796.

58. Pan, X. C.; Malhotra, N.; Simakova, A.; Wang, Z. Y.; Konkolewicz, D.; Matyjaszewski, K., Photoinduced Atom Transfer Radical Polymerization with ppm-Level Cu Catalyst by Visible Light in Aqueous Media. *J. Am. Chem. Soc.* **2015,** *137* (49), 15430-15433.

59. Jones, G. R.; Whitfield, R.; Anastasaki, A.; Haddleton, D. M., Aqueous Copper(II) Photoinduced Polymerization of Acrylates: Low Copper Concentration and the Importance of Sodium Halide Salts. *J. Am. Chem. Soc.* **2016,** *138* (23), 7346-7352.

60. Dolinski, N. D.; Page, Z. A.; Discekici, E. H.; Meis, D.; Lee, I. H.; Jones, G. R.; Whitfield, R.; Pan, X. C.; McCarthy, B. G.; Shanmugam, S.; Kottisch, V.; Fors, B. P.; Boyer, C.; Miyake, G. M.; Matyjaszewski, K.; Haddleton, D. M.; de Alaniz, J. R.; Anastasaki, A.; Hawker, C. J., What Happens in the Dark? Assessing the Temporal Control of Photo-Mediated Controlled Radical Polymerizations. *J. Polym. Sci. Pol. Chem.* **2019,** *57* (3), 268-273.

61. Dadashi-Silab, S.; Matyjaszewski, K., Temporal Control in Atom Transfer Radical Polymerization Using Zerovalent Metals. *Macromolecules* **2018,** *51* (11), 4250-4258.

62. Considering a typical grafting density (σ) of 0.3 chains nm^{-2}, at the lowest catalyst concentration applied of 0.44 M the content of photogenerated Cu^{I}/Me_6TREN species after 1 hour of UV irradiation (Figure S1) is approximately an order of magnitude higher than the amount of alkyl halides in the system. However, for TPMA ligand, the

reduction is much slower and the content of Cu^{I}/TPMA could be comparable or lower than the amount of alkyl halides, as reflected by decrease of the polymerization rate during the off-periods.

For Table of Contents Use Only:

Surface-Initiated Photoinduced ATRP: Mechanism, Oxygen Tolerance and Temporal Control during the Synthesis of Polymer Brushes

Wenqing Yan, Sajjad Dadashi-Silab, Krzysztof Matyjaszewski, Nicholas D. Spencer, Edmondo M. Benetti